

Heat Distribution of Current Output Type Artificial Neural Networks IC for the MEMS Microrobot

Taisuke Tanaka, Yuya Nakata, Kazuki Sugita, Minami Takato, Ken Saito, Fumio Uchikoba
Department of Precision Machinery Engineering College of Science and Technology, Nihon University,
7-24-1, Narashinodai, Funabashi, Chiba, 274-8501, Japan
E-mail: csta13083@g.nihon-u.ac.jp, takato@eme.cst.nihon-u.ac.jp, kensaito@eme.cst.nihon-u.ac.jp,
uchikoba@eme.cst.nihon-u.ac.jp

Abstract

Heat distribution of the artificial neural networks IC developed for controlling microrobots is described in this paper. We measured the temperature distribution of the designed IC using thermography. As a result, it is found that the major heat source is the current mirror part on the IC. However, it was observed that the part of the artificial neural networks also generated the heat. The heat contribution of the artificial neural network part was evaluated. As a result, the temperature rise of the artificial neural networks part on the IC was calculated to be 0.0535°C per second.

Keywords: Microrobot, Artificial neural networks, MEMS, IC

1. Introduction

Insects inhabit the earth from about 300 million years ago. During that process, insects have experienced many environmental changes and have developed biological functions¹. The insect has excellent form and function. Therefore, if it is possible to produce micro robots having functions equivalent to those of the insect, it is considered to be possible that the robot deal with various situations and application in various fields². For example, in the medical field, the microrobot that mimics the peristaltic movement of the insect has been studied³.

The Insect has a flexible control system with a compact moving mechanism and neural networks of the brain. In order to imitate this, we are applying micro electro mechanical systems (MEMS) technology to create the movement mechanism of the microrobot. MEMS technology is based on the integrated circuit (IC) production process. Also, the conventional program control used as a robot control makes it difficult to deal with unknown situations. Therefore, the control method using the artificial neural networks has been expected as

an alternative method of the program control⁴. Neurons of the brain in the living organisms are connected to each other and form networks. By carrying out information transmission using those, the flexible information processing can be performed. By modeling the neuron of the living organism and constructing the artificial neural networks, the robot can judge and execute the required process by themselves like the living organism. We have integrated simple artificial neural networks into a IC and used it as a controlling circuit of the MEMS microrobot⁵. We designed a current output type artificial neural networks IC to drive the MEMS microrobot using shape memory alloy (SMA) for the actuator. In this paper, focusing on heat generation of the artificial neural networks IC, its heat distribution was measured by thermography. We considered the source of the heat generation from the results.

2. Walking control of microrobot

Artificial muscle wires based on SMA are used in the actuator of the robot. The wire shrinks by joule heat of current flow and extends by cooling. Fig. 1 shows the walking mechanism of the microrobot. The walking motion of the microrobot is generated by the rotational motion of the rotor attached with 4 helical artificial muscle wires. The rotational action of the actuator is obtained from current flows through the artificial muscle wire in the order of A to D. Therefore, the rotor rotates and transmits to the link mechanism of the leg portion.

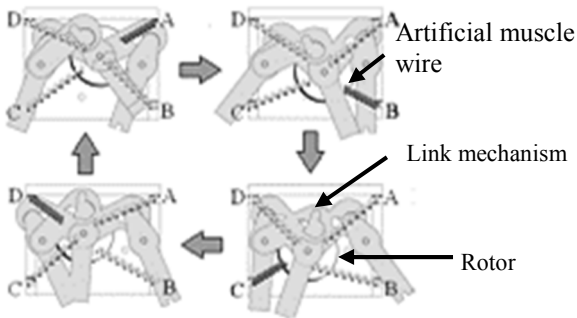


Fig. 1. Walking mechanism of the microrobot.

3. Artificial neural networks

An artificial neural circuit mimics the function of a neural circuit of the living organism with analog electronic circuits. The neural circuits of the living organism is mainly composed of cell bodies, dendrites, axons and synapses. We modeled the cell body and the synapse.

3.1. Cell body model

Fig. 2 shows the circuit diagram of the cell body model. V_C in Fig. 2 is the output voltage. The cell body model consists of a capacitor C_G and a membrane potential capacitor C_M , MOSFETs M_{C1} , M_{C2} , M_{C3} and M_{C4} . The cell body changes the membrane potential using external stimulation and fires electrical pulses. The cell body model has a refractory period, an analog characteristic for the output pulse, and time varying negative resistance characteristics. The circuit parameters for the cell body model were $V_A = 3V$, M_{C1} , M_{C2} : $W/L = 10$, M_{C3} : $W/L = 0.1$, M_{C4} : $W/L = 0.3$, $C_G = 4.7\mu F$, $C_M = 1.0\mu F$.

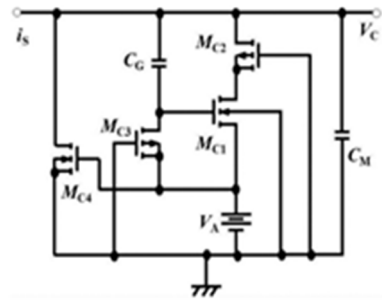


Fig. 2. Circuit diagram of the cell body model.

3.2. Synaptic model

Fig. 3 shows a circuit diagram of an inhibitory synaptic model. When a multiple of cell body models are connected by the synapse model, a synchronization phenomenon occurs at the oscillation timing of the cell body model. The inhibitory synaptic model, particularly, causes anti-phase synchronization. We used the inhibitory mutual coupling to generate driving pulses of the microrobot. The circuit parameters for the inhibitory synaptic model were $V_{DD} = 3V$, $C_{IS1} = 1$ pF, M_{IS1} , M_{IS2} , M_{IS3} , M_{IS4} : $W/L = 1$.

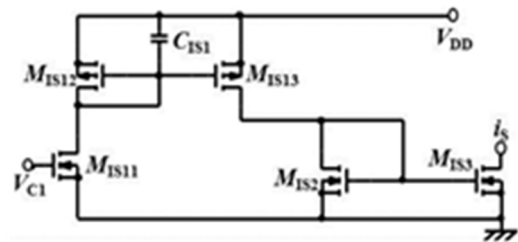


Fig. 3. Circuit diagram of the inhibitory synaptic model.

3.3. Pulse-type hardware neural networks

Fig. 4 shows the pulse-type hardware neural networks mimic a central pattern generator of the living organism. The central pattern generator is known as basic rhythm generator of the living organism. As shown in Fig. 4, four cell body models are inhibitory mutually coupled using 12 inhibitory synaptic models. As a result, a four-phase anti-phase synchronous waveform is generated.

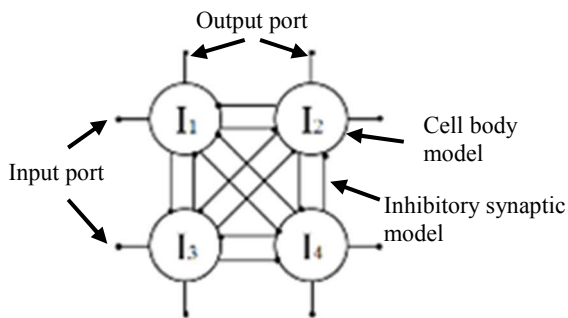


Fig. 4. Pulse-type hardware neural networks.

3.4. Current mirror circuit

Fig. 5 shows a circuit diagram of the current mirror circuit. The shape memory alloy actuator requires the electrical current to generate movement. Therefore, the current mirror circuit is connected to the pulse type hardware neural networks in order to convert the voltage into the current. The circuit parameters for the current mirror circuit were $V_{DD} = 4V$, M_{S1} : $W/L = 40$, M_{S2} : $W/L = 1$, M_{ON} : $W/L = 66$. The number of stages of the current mirror varied by the designed IC.

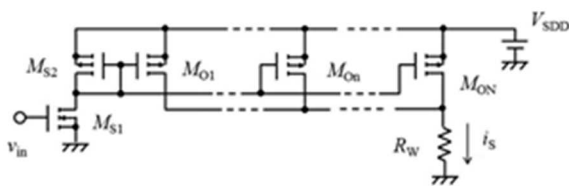


Fig. 5. Circuit diagram of the current mirror circuit.

3.5. Artificial neural networks IC

We designed an IC that constructed pulse-type hardware neural networks. Fig. 6 shows the layout pattern of the designed IC. The design rule of the IC was 4 metal 2 poly CMOS 0.35 μ m. The sizes of the capacitors C_G , C_M of the cell body model were too large to pattern on the IC. Therefore, it was added on the peripheral circuit. Fig. 7 shows an IC mounted on the circuit board. Fig. 8 shows an example of output waveform of the pulse-type hardware neural networks IC.

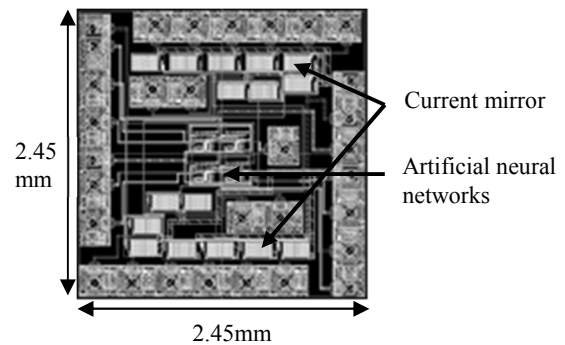


Fig. 6. Layout pattern of Artificial neural networks IC.

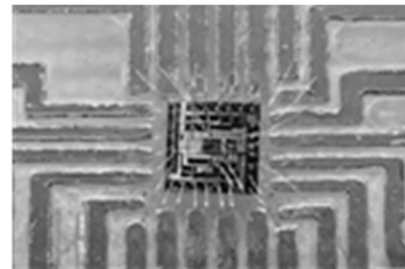


Fig. 7. ICs mounted on the circuit board.

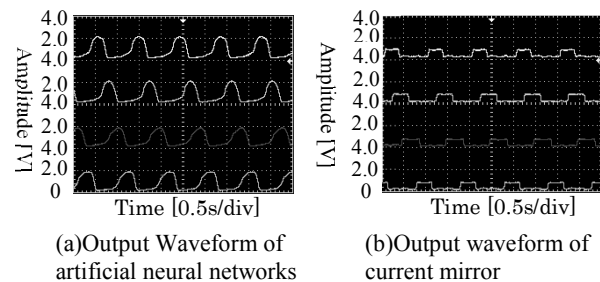


Fig. 8. Example of the output waveform of the pulse type hardware neural networks IC

4. Measurement of heat generation

4.1. Measurement condition

3V was applied to the artificial neural networks using a power source and 4V was applied to the current mirror. A 12 Ω load resistance was connected as output instead of SMA. The measurement was carried out for about 30 seconds after the voltage input. The room temperature was 20°C.

4.2. Measurement result

Fig. 9 shows measurement results. Mainly two high temperature areas are confirmed. The two areas are the artificial neural networks and the current mirror. In the IC shown in Fig. 9, it was confirmed that the maximum temperature in the artificial neural network was 100.4°C and the maximum temperature in the current mirror was 100.1°C.

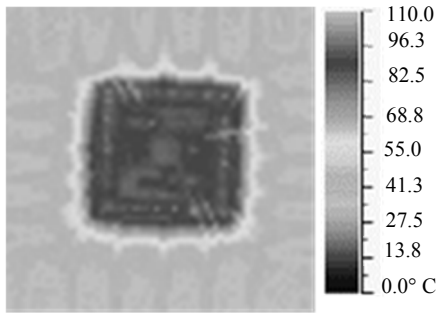


Fig. 9. Temperature distribution measurement on ICs with 12Ω load.

4.3. Measurement result with reduced influence of current mirror

We focused on the heat generation in the artificial neural networks. In order to confirm that the artificial neural network was generating heat, the load resistance was increased from 12Ω to 110Ω. Fig. 10 shows the measurement result. Load resistance of 110Ω was the highest resistance the IC output the stable pulse. In the IC shown in Fig. 10, it was confirmed that the maximum temperature in the artificial neural networks was 39.1°C and the maximum temperature in the current mirror was 39.3°C.

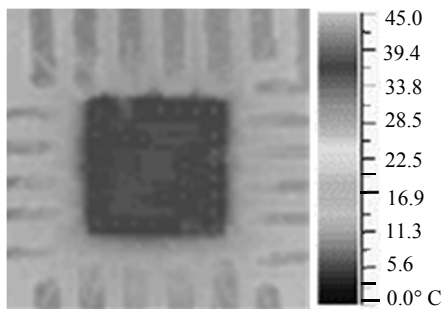


Fig. 10. Temperature distribution measurement on ICs with 110Ω load.

The measurement was performed without applying the power source of the current mirror. In the IC shown in Fig. 11, it was confirmed that the maximum temperature in the artificial neural networks was 29.2°C. Fig. 12 shows the measurement result of the temperature rise at the representative points of the artificial neural networks. The temperature rise in the artificial neural network was confirmed.

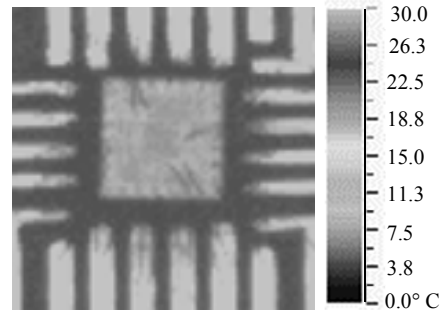


Fig. 11. Measurement of heat distribution of IC without input of current mirror.

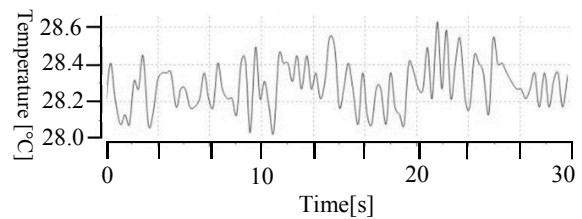


Fig. 12. Measurement result of temperature rise of artificial neural networks.

5. Discussion

5.1. Heat generation in artificial neural networks IC

From these results, it is found that the major heat source is current mirror part because the temperature decreased with increasing of the load resistance. However, the high temperature areas of the IC are corresponding to the not only the current mirror but also the artificial neural networks. The temperature of the artificial neural networks portion was higher than that of the neighbor area. Also, we confirmed the heat generation of the artificial neural network even when the power supply of the current mirror is stopped. The temperature rise almost corresponded to the pulse timing. So, it is suggested the

artificial neural networks also generates the heat to some extends.

5.2. Evaluation of temperature rise per second of artificial neural networks

In the cell body model, when a voltage of V_A is applied, the charge accumulates in C_G , and the potential difference between MOSFETs M_{C1} and M_{C2} disappears. Then, M_{C2} conducts, the charges of C_G and C_M are extracted, applied to the M_{IS3} of the inhibitory synapse model, and flow to GND. It is thought that the heat is generated by the charges extracted from C_G , C_M . We evaluated the calculated value of the temperature rise per second from the power consumption of the capacitors C_G , C_M , the mass of the heat generation part, and the specific heat of silicon. The power consumption due to charges extracted from C_G and C_M can be obtained by equation (1).

$$W = \frac{1}{2} CV^2 [J] \quad (1)$$

C_G and C_M are $4.7\mu\text{F}$ and $1.0\mu\text{F}$ respectively. It is assumed that 0.5 V is applied to C_G and 1.5 V is applied to C_M . Therefore, power consumption of $0.587\mu\text{J}$ and $1.13\mu\text{J}$ are obtained on each capacitor. Because the artificial neural networks is composed of four cell body models, then, the one cycle power consumption of the whole artificial neural networks is calculated as $6.87\mu\text{J}$. The duration of one cycle is 1.1 seconds. Therefore, the total power consumption per second is $6.25\mu\text{W}$. The temperature rise of the artificial neural networks per second can be obtained by equation (2).

$$\Delta T = \frac{P}{\rho V C_V} [^\circ\text{C}] \quad (2)$$

C_V is the specific heat of silicon, 0.73J/gK . V is the volume of heated area. Those are derived from the temperature distribution of the ICs, $6.88 \times 10^{-5}\text{cm}^3$. ρ is the density of the silicon, 2.33g/cm^3 . From these, it is calculated that an artificial neural networks increases 0.0535°C per second. Compared with the calculation result and the measurement result of Fig. 12, the calculated value follows the tendency of the measured value.

© The 2017 International Conference on Artificial Life and Robotics (ICAROB 2017), Jan. 19-22, Seagaia Convention Center, Miyazaki, Japan

6. Conclusion

The heat distribution of the artificial neural networks IC developed to controlling the microrobot was described in this paper. As a result, heat generation was observed with the artificial neural networks and the current mirror parts. It was found that major heat source was the current mirror part. Focusing on the heat generation of artificial neural networks, we thought that heat generated by charges extracted from C_G and C_M of the cell body model. The temperature rise per second was evaluated using the power consumption of C_G and C_M . As a result, it was calculated that the temperature rises of 0.0535°C per second for the IC.

7. References

1. H. Hugo, 2008, *People learn-Insect wisdom*, Tokyo: Tokyo Agricultural University Press Publications
2. A. T. Baisch, P. S. Sreetharan and R. J. Wood, E. H. Miller, Biologically-inspired locomotion of a 2g hexapod robot, in *Proc. Int. Conf. on Intelligent Robots and systems*, (Taipei, Republic of China, 2010), pp. 5360–5365
3. Y. Sonobe, Y. Arai, Y. Nakazato, Development of In-pipe Micro Robot Moving in the Blood Vessel, *Welfare Engineering Symposium Presentation Papers 2007*, (Japan, 2007), pp. 231-232
4. A. Iwata, Y. Amemiya, 1995, Neural network LSI, Tokyo: Institute of Electronics, *Information and Communication Engineers*
5. K. Saito, Y. Ishihara, K. Okane, H. Oku, Y. Asano, K. Iwata, M. Tatani, M. Takato, Y. Sekine and F. Uchikoba, Artificial Neural Circuit Integration for MEMS Microrobot System, in *Proc. 2015 Int. Conf. Advanced Intelligent Mechatronics*, (Busan, Korea, 2015), pp. 1055-1060.